

26 **Abstract**

27 Industrially relevant, commercially available cationic starches have been investigated
28 towards their interaction capacity with cellulose thin films derived from trimethylsilyl
29 cellulose (TMSC). The starches used in this study stem from different sources (potato,
30 pea, corn) and featured rather low degrees of substitution ranging from 0.030 to
31 0.062. The interaction of those starches with cellulose thin films was studied by
32 surface plasmon resonance spectroscopy under flow conditions using concentrations
33 of $1.0 \text{ mg}\cdot\text{ml}^{-1}$ and a flow rate of $25 \text{ }\mu\text{l}\cdot\text{min}^{-1}$. All the investigated starches employed in
34 this study were capable to efficiently interact with the slightly negatively charged
35 cellulose surface leading to irreversible deposition on the surface. As complementary
36 techniques atomic force microscopy and x-ray photoelectron spectroscopy were used
37 to confirm the presence of the starches on the cellulose film surface. Further,
38 dynamic light scattering and size exclusion chromatography measurements were
39 performed to correlate adsorbed amount, particle size and molecular weight of the
40 starches to their interaction behavior.

41

42

43

44

45

46 **Keywords:** cationic starch; cellulose thin films; nanocellulose; surface plasmon
47 resonance

48

49

50

51 **1. Introduction**

52 Cationic polymers are important materials for tailoring the properties of cellulosic
53 substrates such as fibers and pulps. These polyelectrolytes carry a large amount of
54 positive charges on their backbone and are capable to efficiently interact with
55 negatively charged polymers. (Dobrynin, Deshkovski, & Rubinstein, 2001) The
56 cationic polymers very often take the role of adhesion promoters, thereby triggering
57 or enhancing the adsorption of other functional molecules/particles. Consequently,
58 the interaction of many cationic polymers with a variety of cellulosic substrates has
59 been extensively studied in the past. (Geffroy, Labeau, Wong, Cabane, & Cohen
60 Stuart, 2000; Guan, Qian, Xiao, Zheng, & He, 2008; Hasani, Cranston, Westman, &
61 Gray, 2008; K. S. Kontturi et al., 2009; K. S. Kontturi, Tammelin, Johansson, &
62 Stenius, 2008; Lee, Lee, & Youn, 2014; Tamilselvan Mohan et al., 2014; T. Mohan,
63 Ristic, et al., 2013; T. Mohan, Zarth, et al., 2013; Petersen, Radosta, Vorweg, &
64 Kießler, 2013; Schwikal et al., 2011; Terada, Samoshina, Nylander, & Lindman,
65 2004a, 2004b; Yokota, Kitaoka, & Wariishi, 2007) This originates from the importance
66 of cationic polymers in fiber manufacturing processes as well as in papermaking. For
67 instance, cationization of cellulosic textile fibers is often employed to increase anionic
68 dye uptake on and into the fiber matrix. (Nechwatal, Michels, Kosan, & Nicolai, 2004)
69 Further, the deposition of cationic starches has also been proposed to induce
70 antimicrobial action against several microorganisms. (Guan, Qian, Xiao, & Zheng,
71 2008) In contrast, in paper industry the addition of cationic polymers and here in
72 particular of cationic starches is pivotal to produce papers with better retention
73 properties and higher dry strength.(Nachtergaele, 1989) A major issue to unravel the
74 interaction of such cationic starches with cellulosic materials is their intrinsic
75 inhomogeneity (e.g. diameter, morphology, accessibility, composition etc.) which

76 makes it difficult to extract fundamental parameters governing their interaction
77 behavior in real time. Although there are some methods available which can track
78 changes on e.g. fiber matrices such as isothermal titration calorimetry
79 (thermodynamics) and zeta potential (charge) measurements, an elegant way to
80 overcome problems associated with inhomogeneity is to use materials with a well-
81 defined morphology, chemistry and charge.(Rohm, Hirn, Ganser, Teichert, &
82 Schennach, 2014) A particularly well established system has been introduced by
83 Klemm in 1993 and further developed by Kontturi which is based on mostly
84 amorphous cellulose thin films. (E. Kontturi, Thüne, & Niemantsverdriet, 2003;
85 Schaub, Wenz, Wegner, Stein, & Klemm, 1993) These two-dimensionally
86 constrained films can be easily prepared by depositing solutions of a precursor
87 (trimethylsilyl cellulose, TMSC) on a flat surface and by a subsequent spin coating
88 step smooth films are obtained. These silylated cellulose films can be simply
89 converted to cellulose thin films by exposing them to hydrochloric acid vapors over a
90 period of several minutes. Their defined morphology, chemical composition and the
91 homogenous surface allow for a detailed investigation of the surface properties and
92 their interaction with other biomolecules such as proteins, or other polysaccharides.
93 (Niegelhell et al., 2016; Hannes; Orelma, Johansson, Filpponen, Rojas, & Laine,
94 2012; Strasser et al., 2016) In this context, just a few studies focus on how cationic
95 polysaccharides interact with cellulose thin films. Examples include different types of
96 chitosans, cationic celluloses, cationic xylans and also cationic starches. (Lee et al.,
97 2014; Tamilselvan Mohan et al., 2014; T. Mohan, Ristic, et al., 2013; T. Mohan, Zarth,
98 et al., 2013; Hannes Orelma, Filpponen, Johansson, Laine, & Rojas, 2011) In these
99 studies researchers employ cationic starches with different degrees of substitution
100 (0.2-0.75) and focus on whether and to which extent the presence of electrolytes

101 change the interaction capacity with cellulose and as comparison to silica. (K. S.
102 Kontturi et al., 2009; K. S. Kontturi et al., 2008) As for other charged polymers
103 (Geffroy et al., 2000; Hasani et al., 2008; Tammelin, Saarinen, Österberg, & Laine,
104 2006; Yokota et al., 2007) it was demonstrated that the degree of coiling strongly
105 determines the adsorption of the starches onto the surfaces. (Tammelin, Merta,
106 Johansson, & Stenius, 2004) The degree of coiling in turn strongly correlates with the
107 amount of electrolyte in the solutions since it prevents repulsion between individually
108 charged segments by charge screening. Without such a screening the cationic
109 polymers adopt a flat-like, extended conformation usually leading to the formation of
110 thin layers. (Dobrynin et al., 2001; Dobrynin & Rubinstein, 2005) However, the use of
111 starches directly employed for papermaking processes do often have rather low
112 degrees of substitution DS (<0.08). Therefore, the repulsion between the substituted
113 segments is small and can become at a certain point negligible leading to coiled
114 conformations even in the absence of electrolytes. In this study, we aim at a deeper
115 understanding on how such lowly substituted starches interact with cellulose thin
116 films in real time using surface plasmon resonance spectroscopy (SPR). The
117 employed cationic starches are manufactured in large quantities and are intended for
118 papermaking issues. They feature DSs ranging from 0.030 to 0.062.

119

120 **2. Experimental**

121 2.1. Materials

122 Trimethylsilyl cellulose (TMSC, Avicel, $M_w = 185,000 \text{ g}\cdot\text{mol}^{-1}$, $M_n = 30,400 \text{ g}\cdot\text{mol}^{-1}$,
123 PDI = 6.1 determined by SEC in chloroform) with a DS_{Si} value of 2.8-2.9 was
124 purchased from TITK (Rudolstadt, Germany). SPR gold sensor slides (CEN102AU)
125 were purchased from Cenibra, Germany. Milli-Q water (resistivity = $18.2 \text{ M}\Omega^{-1}\cdot\text{cm}^{-1}$)

126 from a Millipore water purification system (Millipore, USA) was used for contact angle
127 determinations and SPR experiments. Chloroform (99.3%), hydrochloric acid (37%),
128 hydrogen peroxide (30% in water) and sulfuric acid (95%) were purchased from
129 Sigma Aldrich and used as received. Wet end starches commonly used in paper
130 production were used without further purification. Cationic starches were cooked at
131 appropriate temperatures (95-125°C).

132

133 2.2. Substrate Cleaning and Film Preparation.

134 Prior to spin coating, SPR gold sensor slides/silicon wafers were immersed in a
135 “piranha” solution containing H₂O₂ (30 wt.%)/H₂SO₄ (1:3 v/v) for 10 min, then
136 extensively rinsed with MilliQ water and blow dried with N₂ gas. 100 µl of a TMSC
137 solution (0.75 wt% in chloroform) were deposited onto the substrate and then rotated
138 for 60 s at a spinning speed of 4000 rpm and an acceleration of 2500 rpm·s⁻¹. To
139 convert TMSC into pure cellulose, the sensors/wafers were placed in a polystyrene
140 petri-dish (5 cm in diameter) containing 3 ml of 10 wt.% hydrochloric acid (HCl). The
141 dish was covered with its cap and the films were exposed to the vapors of HCl for 12
142 min. The regeneration of cellulose from TMSC was verified by water contact angle
143 **(Figure S1)** and ATR-IR **(Figure S2)** measurements as reported elsewhere.
144 (Tamilselvan Mohan et al., 2012; T. Mohan et al., 2012)

145

146 2.3. Multi Parameter Surface Plasmon Resonance Spectroscopy – MP-SPR.

147 MP-SPR spectroscopy was accomplished with a SPR Navi 200 from Bionavis Ltd.,
148 Tampere, Finland, equipped with two different lasers (670 and 785 nm) in both
149 measurement channels, using gold coated glass slides as substrate (gold layer 50

150 nm, chromium adhesion layer 10 nm). All measurements were performed using a full
151 angular scan (39–78°, scan speed: 8°·s⁻¹).

152 For the adsorption experiments, solutions of cationic starches have been prepared by
153 heating dispersions with a concentration of 1 mg·ml⁻¹ (bone-dry substance) over a
154 period of one hour at 95°C. The resulting clear solutions were then directly used for
155 the adsorption experiments. For the adsorption experiments, the cellulose thin films
156 were allowed to equilibrate for 45 minutes before a continuous flow of the starch
157 solutions was pumped through. The starches were allowed to adsorb for 10 minutes
158 (flow rate 25 µl·min⁻¹). Afterward, the surfaces have been rinsed with MilliQ water to
159 remove loosely bound material.

160 The adsorption of cationic starches onto the cellulose surfaces was quantified
161 according to equation 1, which considers the dependence of the angular response of
162 the surface plasmon resonance in dependence of the refractive index increment
163 (dn/dc) of the adsorbing layer.

$$164 \quad \Gamma = \frac{\Delta\Theta \times k \times d_p}{dn/dc} \quad (1)$$

165 For thin layers (<100 nm), $k \times d_p$ can be considered constant and can be obtained by
166 calibration of the instrument by determination of the decay wave length λ_d . For the
167 SPR Navi 200 used in this study, $k \times d_p$ values are approximately $1.09 \cdot 10^{-7}$ cm/° (at
168 670 nm) and $1.9 \cdot 10^{-7}$ cm/° (at 785 nm) in aqueous systems. Since the degree of
169 substitution of the starches is very low, dn/dc values for native starches have been
170 used ($0.150 \text{ cm}^3 \cdot \text{g}^{-1}$) to determine the amount of adsorbed masses. (Theisen, Johann,
171 Deacon, & Harding, 2000)

172

173 2.4. Dynamic Light Scattering

174 The DLS equipment consisted of a diode laser (Coherent Verdi V5, $\lambda = 532$ nm) and a
175 goniometer with single-mode fiber detection optics (OZ from GMP, Zürich,
176 Switzerland). The data was acquired by an ALV/SO-SIPD/DUAL photomultiplier with
177 pseudo-cross correlation and an ALV 7004 Digital Multiple Tau Real Time Correlator
178 (ALV, Langen, Germany). The correlation functions were determined and stored by
179 the ALV software package. The light scattering (LS) was measured ten times 30 s at
180 a scattering angle of 90° at 25°C and the resulting correlation functions were
181 averaged. The hydrodynamic radius was calculated by the optimized regulation
182 technique software (Schnablegger & Glatter, 1991) by means of the cumulant
183 method. (Koppel, 1972) All cationic starch solutions have been centrifuged at 4000
184 rpm for 30 s prior to measurements.

185

186 2.5. Atomic Force Microscopy – AFM.

187 Surface morphology and roughness of the N_2 -dried films were obtained in tapping
188 mode in ambient atmosphere at room temperature by a Veeco Multimode QuadraX
189 MM scanning probe microscope (Bruker; Billerica, MA, USA) using Si-cantilevers
190 (NCH-VS1-W from NanoWorld AG, Neuchatel, Switzerland) with a resonance
191 frequency of 320 kHz and a force constant of $42 \text{ N}\cdot\text{m}^{-1}$. Root mean square (RMS)
192 roughness calculation and image processing was performed with the Nanoscope
193 software (V7.30r1sr3, Veeco).

194

195 2.6. X-ray photoelectron spectroscopy

196 XPS spectra were recorded using a Thermo Scientific instrument equipped with a
197 monochromatic Al-K α X-ray source (1486.6 eV). High resolution scans were acquired
198 at a pass energy of 50 eV and a step size (resolution) of 0.1 eV. Wide scans were

199 acquired with a pass energy of 100 eV and a step size of 1.0 eV. Photo-electrons
200 were collected using a take-off angle of 90 ° relative to the sample surface. Charge
201 compensation was performed with an argon flood gun. All analyses were performed
202 at room temperature.

203

204 2.7. Size Exclusion Chromatography (SEC).

205 Size exclusion chromatography was performed on a SEC-3010 equipped with an
206 autosampler, a pump with degasser and a refractive index detector from WGE Dr.
207 Bures (Dallgow, Germany). Two analytical columns from AppliChrom (ABOA CatPhil
208 P-350 300 mm × 8 mm) were used at a flow rate of 1 ml·min⁻¹. The temperature of
209 the column oven was set to 30 °C. 0.1 M NaNO₃ was used as eluent. The calibration
210 curve was made with pullulan standards purchased from PSS (Mainz, Germany) with
211 molar masses ranging from 1,080 g·mol⁻¹ to 708,000 g·mol⁻¹.

212

213 2.8. Contact Angle (CA) and Surface Free Energy (SFE) Determination.

214 Static contact angle measurements were performed with a Drop Shape Analysis
215 System DSA100 (Krüss GmbH, Hamburg, Germany) with a T1E CCD video camera
216 (25 fps) and the DSA1 v 1.90 software. Measurements were done with MilliQ water
217 and di-iodomethane using a droplet size of 3 µl and a dispense rate of 400 µl·min⁻¹.
218 For these experiments ex-situ coated silicon wafers have been used since the
219 adsorption slot of the SPR slides is just a few mm². The ex-situ adsorption was
220 performed in a similar manner as the in situ experiments using SPR. This involved
221 the swelling of the films in water for 45 minutes (deposition of ca 500 µl MilliQ water
222 on a 1 cm × 2 cm cellulose coated silicon wafer), then the water was exchanged by
223 the cationic starch solutions (1 mg·ml⁻¹) and allowed to adsorb for 10 minutes.

224 Afterwards, the samples were rinsed with 500 ml of MilliQ water and dried in air
 225 overnight at ambient temperatures. All measurements were performed at least 3
 226 times. SCA were calculated with the Young-Laplace equation and the SFE was
 227 determined with the Owen-Wendt-Rabel-Kaelble (OWRK) method. (Kaelble, 1970;
 228 Owens & Wendt, 1969; Rabel, 1971)

229

230 3. Results and discussion

231 For the determination of the interaction capacity with cellulose thin films, different
 232 industrially relevant cationic starches (CS) were selected which feature very low
 233 degrees of substitution (0.030-0.062). As samples four different starches from
 234 different origins as well as a blend of two starches have been chosen for this study
 235 (Table 1).

236 **Table 1.** List of cationic starches used in this study including information on source,
 237 dry solids content, degree of substitution (DS) and molecular weight.

Source	Label	Dry Solids Content [%]	DS ^a	M _n [g·mol ⁻¹]	M _w [g·mol ⁻¹]	PDI
corn	A	87.3	0.058	7.7 × 10 ⁴	1.7 × 10 ⁵	2.18
potato	B	83.9	0.030-0.036	4.3 × 10 ⁵	1.4 × 10 ⁶	3.20
corn, potato	Blend A:B 80:20	85.2	0.050-0.056	n.d.	n.d.	n.d.
pea	C	81.9	0.047	3.7 × 10 ⁵	7.4 × 10 ⁵	1.99
waxy corn	D	86.9	0.062	1.3 × 10 ⁶	2.4 × 10 ⁶	1.94

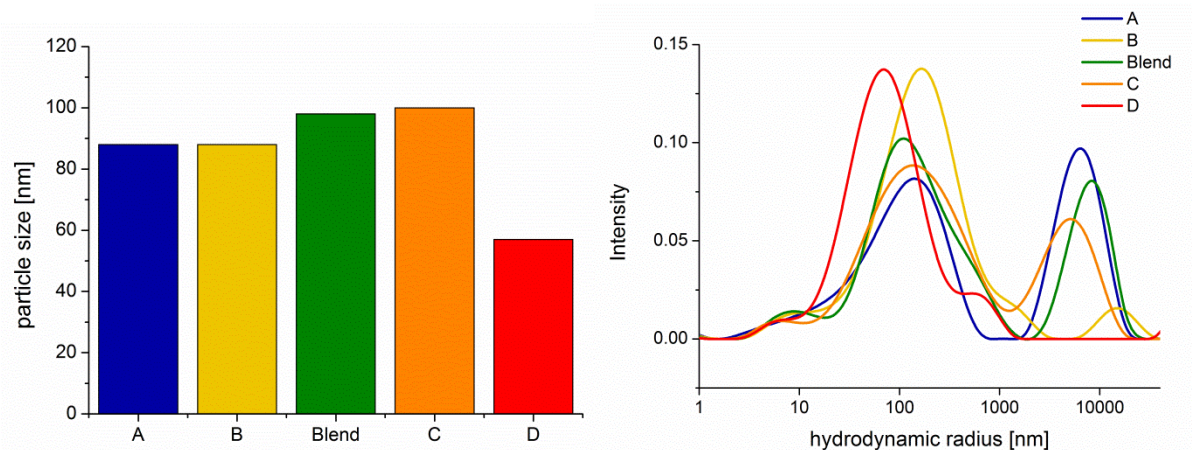
238 ^a According to the manufacturer. (n.d. non determined)

239 Since the investigated starches do not completely dissolve at room temperature in
 240 water, they were cooked at appropriate temperatures (95-125°C, 1 mg·ml⁻¹ bone-dry

241 substance) over a period of 60 minutes to obtain macroscopically clear solutions
242 suitable for adsorption experiments. It should be noted here that all the starches have
243 been used at their native pH values (5.0-5.8) (**Table S1**); any adjustment of pH value
244 or addition of electrolytes was intentionally avoided for this study. These
245 macroscopically clear solutions were investigated by size exclusion chromatography
246 and dynamic light scattering after cooling to room temperature. Size exclusion
247 chromatography results are in agreement with literature, where molar masses of
248 approximately 10^5 - 10^6 g·mol⁻¹ and 10^7 - 10^8 g·mol⁻¹, have been determined for
249 amylose and amylopectin respectively. (Banks & Greenwood, 1975) In general, waxy
250 corn starches feature amylose contents of maximum 1% (Pérez & Bertoft, 2010) and
251 therefore CS D displays the highest molar mass of the herein studied starches
252 concomitant with a small polydispersity index. Starches containing relatively high
253 amylose contents, such as pea starch (40-70%) and corn starch (30 %) feature lower
254 molar masses compared to starches derived from waxy corn or potato (20% amylose
255 content). (McCready, Guggolz, Silviera, & Owens, 1950; Rosin, Lajolo, & Menezes,
256 2002)

257 As depicted in **Figure 1**, all of the investigated starches form particles with a size
258 (median hydrodynamic diameter) ranging from 57 (CS D) to 100 nm (Blend, CS C).
259 However, the size distribution is at least of bimodal nature and shows larger particles
260 (micron range) as well as very small particles with a size of ca 10 nm. It is important
261 to point out that particles with larger size lead to a response with higher intensity than
262 smaller particles. Interestingly, there are not any particles in the micron range size
263 present for the starch solutions consisting mostly of amylopectin (CS D). It could be
264 concluded that the large particles present in solutions of the other compounds (CS A,
265 B, and C) are composed of starch clusters formed by aggregation of amylose and

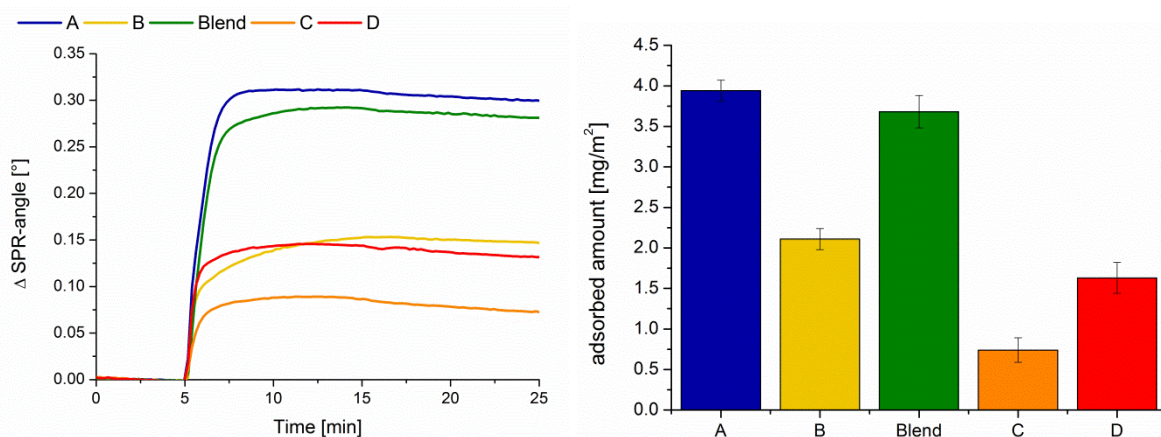
266 amylopectin. (Shirazi, van de Ven, & Garnier, 2003a) Although amylopectin is the
267 starch component with higher molecular weight, it is of branched nature and therefore
268 the hydrodynamic radius is smaller for CS D than for the other starches containing
269 non-branched amylose.



270
271 **Figure 1.** Left: Comparison of the median particle size of the different cationic
272 starches in aqueous solution ($c = 1 \text{ mg}\cdot\text{mL}^{-1}$) determined by DLS in the 57-100 nm
273 regime. Right: Intensity weighted size distribution of the cationic starch solutions
274 obtained by DLS.

275 For adsorption experiments using surface plasmon resonance spectroscopy, the
276 same dissolution procedure was applied as for the samples used in SEC and DLS
277 experiments. These adsorption experiments were designed in way that after
278 equilibration of the cellulose thin films over a period of 45 minutes in water, the
279 cationic starches were pumped through the microfluidic channel and allowed to
280 interact until a plateau was reached (i.e. after 10 minutes). Afterwards, the samples
281 were rinsed with water in order to remove loosely bound materials from the cellulose
282 thin films. The change in the surface plasmon resonance angle is then used to
283 determine the amount of deposited cationic starches onto the surfaces according to
284 equation (1).

285 As depicted in **Figure 2**, the cationic starches irreversibly adsorb onto the cellulose
286 thin films and a final rinsing step did not remove a significant amount of material from
287 any of the films. This can be attributed to reorientation of the adsorbed molecules as well,
288 well, since SPR detects changes in refractive index which is traceable to adsorption,
289 desorption or density variations. Furthermore, adsorption occurs spontaneously and
290 kinetics is fast, demonstrating a high affinity of the CS to the cellulose films. However,
291 the extent of adsorption strongly varies for all the investigated samples ranging from
292 0.74 ± 0.15 (CS D) to ca. $3.94 \pm 0.13 \text{ mg}\cdot\text{m}^{-2}$ (CS A). An exception in terms of
293 kinetics is the starch B sample whose adsorption profile is much slower than for all
294 the other investigated samples. Factors governing the kinetics in the adsorption of
295 polymers can be related to molecular weight and to the PDI, to mention just two
296 parameters. It is known from literature that a polymer with higher PDI is prone to
297 slower adsorption than the same polymer with a smaller PDI. Interestingly, the PDI is
298 the highest for CS B sample which could be the reason for the rather slow adsorption
299 on cellulose thin films. (Kronberg, Holmberg, & Lindman, 2014) This phenomenon
300 initially proven for proteins and often recalled the Vroman effect, relates to species
301 with a lower molar mass which are slowly replaced by those with a higher mass,
302 thereby causing much slower kinetics.



303

304 **Figure 2.** Comparison of the adsorption behavior of the different starches ($c= 1$
305 $\text{mg}\cdot\text{ml}^{-1}$, flow rate $25 \mu\text{l}\cdot\text{min}^{-1}$) as a function of the SPR angle (left) and corresponding
306 adsorbed masses (right).

307

308 A similar behavior is observed for the blend of CS A and CS B (80:20). Here, the
309 extent of adsorbed material ($3.68 \pm 0.2 \text{ mg}\cdot\text{m}^{-2}$) matches the calculated value of the
310 individual components ($3.57 \pm 0.13 \text{ mg}\cdot\text{m}^{-2}$) but the adsorption kinetics is rather
311 different. In the beginning of the adsorption experiment, the blend behaves like CS A
312 (same slope) with a very fast adsorption rate. However, after 2 minutes the slope of
313 the curve becomes less steep i.e. the adsorption is slower and proceeds in a similar
314 fashion as the curve of CS B. As for the CS B adsorption, the fraction with higher
315 molar mass slowly replaces those with lower molar mass as mentioned in literature
316 for other polymer blends having different molar masses. (Dijt, Cohen Stuart, & Fler,
317 1994; Fu & Santore, 1998)

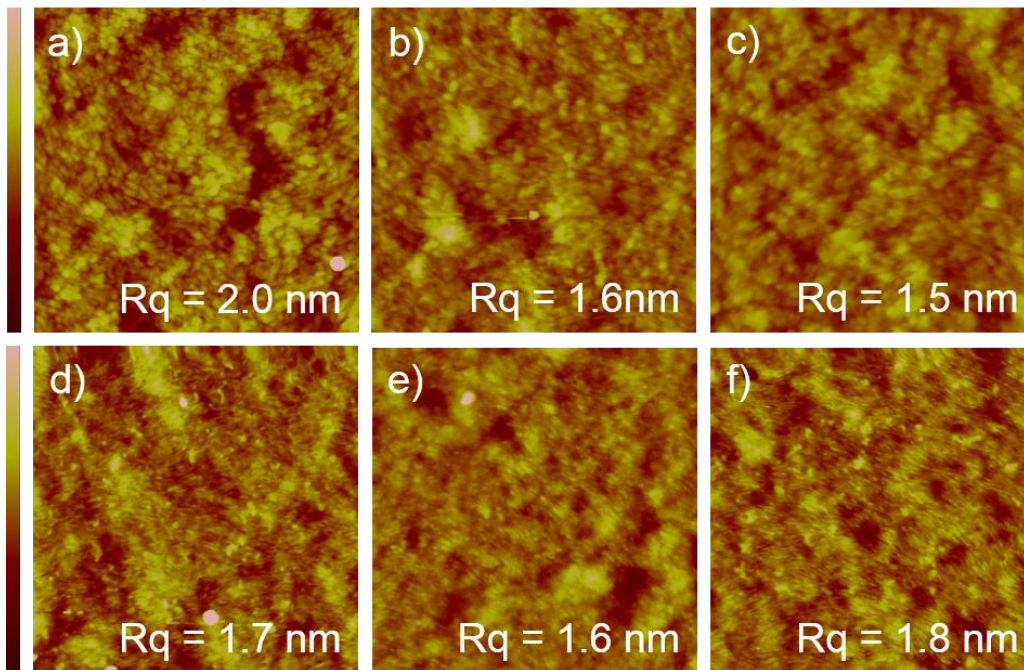
318 After drying in air at room temperature, the same films from SPR experiments were
319 subjected to XPS measurements to confirm the presence of nitrogen stemming from
320 the cationically charged groups (i.e. ammonium groups) in CS on the cellulose films.
321 The XPS results are shown in **Table 2** and clearly show the presence of the cationic
322 species on those films exposed to CS solutions whereas the neat cellulose films do
323 not contain any nitrogen. However, a quantitative assessment using XPS is not
324 always straightforward since the recorded intensities depend on several parameters
325 e.g. the homogeneous distribution of starch particles throughout the sample. Besides
326 the N_{1s} also the Cl_{2p} signal is observed, which relates to the chloride counterion and
327 matches the nitrogen content. Carbon and oxygen signals arise from the backbone of
328 starch and the underlying cellulose layer, which is plausible since even some signal

329 originating from the gold substrate is detectable to a minor extent. The full survey
330 scans are available in the Supporting Materials (**Figure S1-S6**).

331 **Table 2.** Elemental composition (atom%) of the pure and cationically modified
332 cellulose films determined by XPS.

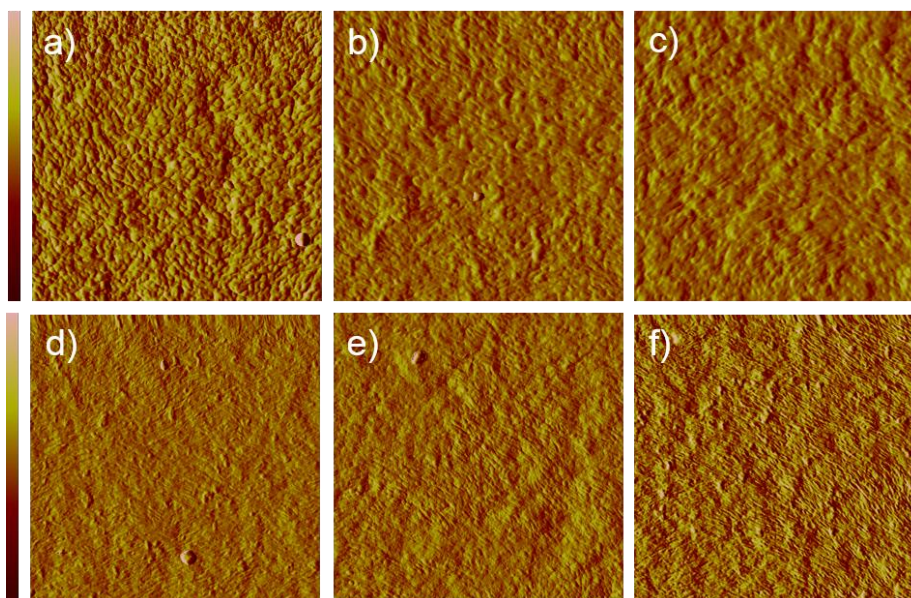
	atom%					
	Cellulose	A	B	blend	C	D
C _{1s}	58.1	59.4	58.9	59.2	59.1	59.2
O _{1s}	38.0	36.8	38.5	37.9	39.0	38.9
N _{1s}	<LOD	0.8	1.1	1.1	0.9	1.0
Cl _{2p}	<0.5	1.0	0.9	0.9	0.8	1.0

333
334 Further, the SPR samples were subjected to atomic force microscopy. The
335 topography images (**Figure 3**) do not exhibit large differences between the different
336 samples before and after adsorption, albeit a decrease in surface roughness is
337 observed after CS adsorption. This can be explained by cationic starch particles
338 filling the pores and holes present on the cellulose thin film. Despite the similar
339 chemical nature of adsorbents and the cellulose surface, the amplitude images
340 provide (**Figure 4**) better insights. In those images, it can be clearly seen that larger
341 particulates are present for CS A and the blend, whereas for the other samples rather
342 small features are present. The size of these features is in good agreement with the
343 results obtained by DLS, where both, CS A and the blend, feature a bimodal size
344 distribution with some large particles. CS C displays aggregates with large particles
345 size too, however, the amount deposited on the cellulose films is rather low to be
346 detected by AFM.



347

348 **Figure 3.** Comparison of AFM topography images ($1 \times 1 \mu\text{m}^2$, z-scale 20 nm) of the
 349 different samples before (a) and after adsorption (b-f). b: CS A, c: CS B, d: blend, e:
 350 CS C, f: CS D. All samples have been measured in air at ambient atmosphere.

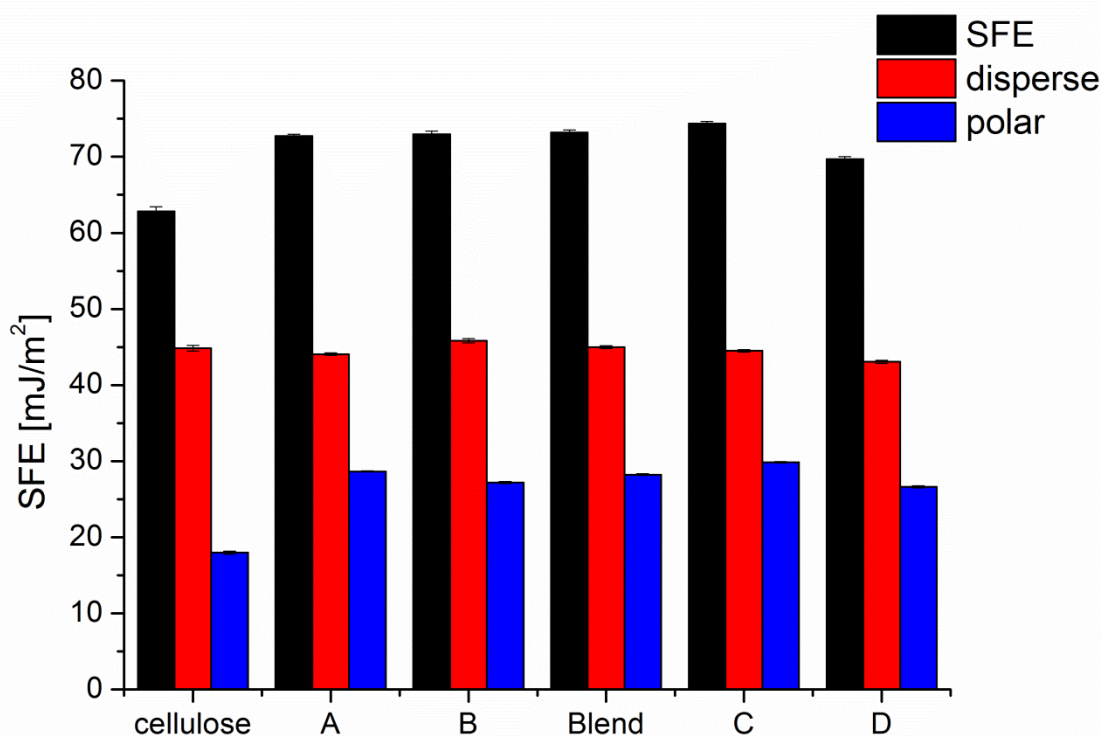


351

352 **Figure 4.** Comparison of AFM amplitude images ($1 \times 1 \mu\text{m}^2$, z-scale 10mV) of the
 353 different samples before (a) and after adsorption (b-f). b: CS A, c: CS B, d: blend, e:
 354 CS C, f: CS D. All samples have been measured in air at ambient atmosphere.

355

356 The modification of a surface by a charged polymer should impact the hydrophilicity
357 of the surface to some extent as well. The surface free energies of the films,
358 determined by wettability studies using water and diiodomethane, increased after the
359 deposition of the cationic starches on the surfaces (**Figure 5**). However, the increase
360 in SFE does not significantly relate to the amount of cationic starch deposited on the
361 surface and SFEs in the range of $70 \text{ mJ}\cdot\text{m}^{-2}$ have been determined. Only for the
362 sample with the lowest affinity, a slightly lower SFE was observed. However, even for
363 the CS with a rather low affinity to the surface, the SFE increased compared to
364 cellulose ($67 \text{ mJ}\cdot\text{m}^{-2}$ for CS D vs. $62 \text{ mJ}\cdot\text{m}^{-2}$ for cellulose). The increase in SFE can
365 be mainly attributed to higher polar contributions to SFE in the case of CS compared
366 to cellulose.



367
368 **Figure 5.** Comparison of the SFE of non-modified cellulose thin films and those
369 modified with CS.

370 The results can be rationalized in following respects. The interaction of any type of
371 polymer with a surface is governed by the properties of the individual components
372 (e.g. charge density), the conformation of the adsorbens (flat vs. coiled) and the
373 solubility of the polymer at the interface.(Dobrynin & Rubinstein, 2005) The SPR data
374 shows significant differences in the interaction capacity of cellulose thin films with
375 different cationic starches. These differences depend partially on the charge of the
376 substrate and the adsorbens. However, for the industrially relevant CS, the amount of
377 cationic groups is rather low. When considering an average length of 0.5 nm of an
378 anhydrous glucose unit (AGU), the mean distance between the charges ranges from
379 8 to 15 nm for the CS with the lowest and highest DS, respectively. Considering the
380 molecular weights of the different compounds employed in this study, the amount of
381 charged groups that are present on the polymer backbone were calculated and are
382 shown in **Table 3**. The calculations assume perfectly flat, non aggregated starch
383 molecules and neither take into account the uneven distribution of the cationic groups
384 within the starch molecules nor the difference in cationization of amylose and
385 amylopectin within the type of CS. In general, amylose is better accessible for
386 cationic modification than amylopectin leading to a higher DS. (Steeneken & Smith,
387 1991) Despite the low mean number of charges per molecule compared to cationic
388 starches with higher degree of substitution, a relatively high interaction capacity is
389 found for the starches applied in this study. In terms of nitrogen content determined
390 by XPS, all the modified cellulose featured higher N contents than those reported in
391 literature where many CS with higher DS had been used (0.2 and 0.75). (K. S.
392 Kontturi et al., 2008)

393 **Table 3.** Mean distance between charges, mean length of starch molecules and
394 number of cationic charges present on the polymer backbone in an extended flat
395 conformation of different CS calculated from molecular weights and DS.

	mean distance charges [nm]	mean length molecule [nm]	mean number of charges
A	8.6	376	44
B	15.2	2810	185
Blend	9.4	3514	372
C	10.6	1715	161
D	8.1	5690	706

396
397 Results from cationic starches with the same particle size reveal the influence of the
398 DS and the amount of cationic charges at the polymer backbone. For instance, CS A
399 ($3.94 \pm 0.13 \text{ mg}\cdot\text{m}^{-2}$) and CS B ($2.11 \pm 0.13 \text{ mg}\cdot\text{m}^{-2}$) features the same particle size,
400 but a different DS. Higher DS basically leads to more electrostatic attraction between
401 the cellulosic substrate and the compound leading to more pronounced interaction
402 and finally adsorption. Additionally, CS A and CS B have a similar content of amylose,
403 therefore the uneven distribution of cationic charges between amylose and
404 amylopectin can be considered negligible. This effect is observed for the blend (3.68
405 $\pm 0.2 \text{ mg}\cdot\text{m}^{-2}$) and CS C ($0.74 \pm 0.15 \text{ mg}\cdot\text{m}^{-2}$) as well. In this case, the amylose
406 content differs, which may have an effect in the adsorption behavior.
407 CS B and CS C (**Table 3**) exhibit different adsorption capacities on the cellulose films,
408 even though they contain a similar amount of cationic charges. Interestingly, the
409 compound with the higher DS (CS C) adsorbs to a lesser extent, whereby the
410 adsorbed amount of the CS that forms the smaller aggregates (CS B) is more than
411 twice as high. This indicates that besides the DS, additional factors influence the
412 adsorption behavior of the cationic starches. One of these factors is the solubility of
413 the polymers which is dependent on molecular weight, the amylose/amylopectin ratio

414 and the charge. (Kronberg et al., 2014) Polymer solubility increases with the amount
415 of charges on a polyelectrolyte leading to lower adsorption. However, this is in
416 contradiction with the electrostatic interaction between adsorbens and substrate,
417 since a high DS favors electrostatic attraction to the negatively charged cellulose
418 substrate (ζ -potential ca. -18 mV at pH 5-6 (Ristić et al., 2014)). This phenomenon is
419 observed for compounds with the same particle size, such as CS A and CS B or the
420 blend and CS C, where electrostatic attraction is overruled by solubility. Besides
421 charge, molecular weight and particle size control the solubility. In principle, low
422 molecular weight polymers are better soluble than those with high molecular weight,
423 therefore large molecules tend to adsorb in larger amounts but - as already
424 discussed above - slower. The same effect applies for particle sizes. Different
425 observations have been made by Shirazi and coworkers, who investigated the
426 adsorption of cationic starches on pulp fibers. (Shirazi, van de Ven, & Garnier,
427 2003b) They proposed an initial adsorption step of starch aggregates followed by a
428 deposition of individual macromolecules onto the cellulose fiber surface.

429 The influence of particle hydrodynamic radius can be illustrated by comparing CS A
430 (88 nm), the blend (98 nm) and CS D (57 nm), all having a similar DS. Compared to
431 CS D for instance, larger amounts of CS A and the blend (compared to CS D) adsorb
432 onto the cellulose films since larger particles are less soluble and tend to adsorb to a
433 higher extent. Moreover, conformation and the resulting availability of attachment
434 sites are decisive factors as well. As seen in the above mentioned case of CS C and
435 CS B, this parameter is important and can be ascribed to the amylose content of the
436 starches. Since amylose is the low molecular polymer in starch and is better
437 accessible to the cationization procedure than amylopectin, therefore featuring a
438 higher DS, the amylose proportion of the cationic starch keeps dissolved while larger

439 starch clusters adsorb. CS D, the cationic starch with the highest molecular weight
440 and amylopectin content, displays theoretically the highest amount of charges (~706)
441 present on the polymer backbone. However, due to the conformation of amylopectin,
442 fewer charges are accessible for interaction with the surface. (Shirazi et al., 2003b;
443 Swerin & Wågberg, 1994) The branched structure of amylopectin permits less
444 freedom in chain movement and does not easily rearrange compared to amylose. In
445 addition to that, CS D forms rather small particles, thereby increasing their solubility.
446 Of course ionic strength is an essential parameter in the interaction of oppositely
447 charged materials, because it impacts conformation by charge screening. Although
448 the investigation of the influence of ionic strength on the adsorption behavior was not
449 the main focus of this work, for the sake of comparison one sample (CS B) was
450 selected and adsorbed at different electrolyte concentrations (1 mM, 10mM, 100 mM
451 NaCl) in the same SPR setup as for the other samples. The results are summarized
452 in **Figure S8-S12**. Results follow the expected trends and fit to data reported in
453 literature. (Shirazi et al., 2003b) The particle size of CS B decreases upon addition of
454 salt to the CS solution from 88 nm (pure water) to approximately 75 nm due to
455 screening of the positive charges and reduction of electrostatic repulsion in the
456 polymer. The increase of the ionic strength to 1 mM NaCl leads to a higher extent of
457 adsorption. However, a further increase in salt concentration does not only decrease
458 intramolecular repulsion but the surface-starch interactions are screened too, leading
459 to even smaller adsorbed amounts of CS B than in pure water.

460

461 **4. Conclusion**

462 In summary, the adsorption behavior of industrially relevant cationic starches with low
463 degrees of substitution (0.03-0.06) on cellulose thin films was investigated in the

464 absence of any electrolytes and at native pH value of the starches. It turned out that
465 all the investigated starches irreversibly adsorb onto cellulose, whereas the extent of
466 mass deposited on the surfaces varies from ca 0.7 to ca 4.0 mg·m⁻². For CS with the
467 same size, the adsorption capacity is mainly influenced by the DS. For those CS, a
468 high DS leads to higher deposition on the surface. In these cases, electrostatic
469 interactions overcome solubility of the polymers. When it comes to starches with very
470 similar DS, the particle size dominates adsorption, since smaller particles are better
471 soluble and therefore adsorb to a lesser extent. Another crucial factor is the
472 conformation of the polymer and concomitant the availability of attachment sites,
473 which is among others dependent on the amylose-amylopectin ratio of the starch. In
474 conclusion, cationic starch adsorption behavior is primarily governed by the interplay
475 of solubility and electrostatic interaction which are both influenced by different
476 parameters such as particle size, molecular weight, conformation and DS. The
477 influence of the substrate's negative charge stemming from partial oxidation i.e.
478 carboxylic groups on the adsorption behavior of cationic compounds is an additional
479 factor, which is certainly critical for industrial materials featuring various degrees of
480 oxidation. Currently, we are investigating whether these results are transferable to
481 industrially manufactured materials such as fibers and papers.

482

483 **Acknowledgement**

484 The financial support of the Federal Ministry of Economy, Family and Youth and the
485 National Foundation for Research, Technology and Development, Austria, is
486 gratefully acknowledged.

487

488 **References**

- 490 Banks, W., & Greenwood, C. T. (1975). *Starch and its Components*. New York: Wiley.
- 491 Dijt, J. C., Cohen Stuart, M. A., & Fleer, G. J. (1994). Competitive Adsorption Kinetics of
492 Polymers Differing in Length Only. *Macromolecules*, 27(12), 3219-3228.
- 493 Dobrynin, A. V., Deshkovski, A., & Rubinstein, M. (2001). Adsorption of Polyelectrolytes at
494 Oppositely Charged Surfaces. *Macromolecules*, 34(10), 3421-3436.
- 495 Dobrynin, A. V., & Rubinstein, M. (2005). Theory of polyelectrolytes in solutions and at
496 surfaces. *Progress in Polymer Science*, 30(11), 1049-1118.
- 497 Fu, Z., & Santore, M. M. (1998). Competitive Adsorption of Poly(ethylene oxide) Chains
498 with and without Charged End Groups. *Langmuir*, 14(15), 4300-4307.
- 499 Geffroy, C., Labeau, M. P., Wong, K., Cabane, B., & Cohen Stuart, M. A. (2000). Kinetics of
500 adsorption of polyvinylamine onto cellulose. *Colloids and Surfaces A:
501 Physicochemical and Engineering Aspects*, 172(1-3), 47-56.
- 502 Guan, Y., Qian, L., Xiao, H., & Zheng, A. (2008). Preparation of novel antimicrobial-
503 modified starch and its adsorption on cellulose fibers: Part I. Optimization of synthetic
504 conditions and antimicrobial activities. *Cellulose*, 15(4), 609-618.
- 505 Guan, Y., Qian, L., Xiao, H., Zheng, A., & He, B. (2008). Synthesis of a novel antimicrobial-
506 modified starch and its adsorption on cellulose fibers: part II—adsorption behaviors of
507 cationic starch on cellulose fibers. *Cellulose*, 15(4), 619-629.
- 508 Hasani, M., Cranston, E. D., Westman, G., & Gray, D. G. (2008). Cationic Surface
509 Functionalization of Cellulose Nanocrystals. *Soft Matter*, 4, 2238-2244.
- 510 Kaelble, D. H. (1970). Dispersion-Polar Surface Tension Properties of Organic Solids. *J.
511 Adhes.*, 2, 66-81.
- 512 Kontturi, E., Thüne, P. C., & Niemantsverdriet, J. W. (2003). Cellulose Model Surfaces
513 Simplified Preparation by Spin Coating and Characterization by X-ray Photoelectron
514 Spectroscopy, Infrared Spectroscopy, and Atomic Force Microscopy. *Langmuir*,
515 19(14), 5735-5741.
- 516 Kontturi, K. S., Holappa, S., Kontturi, E., Johansson, L.-S., Hyvärinen, S., Peltonen, S., &
517 Laine, J. (2009). Arrangements of cationic starch of varying hydrophobicity on
518 hydrophilic and hydrophobic surfaces. *Journal of Colloid and Interface Science*,
519 336(1), 21-29.
- 520 Kontturi, K. S., Tammelin, T., Johansson, L.-S., & Stenius, P. (2008). Adsorption of Cationic
521 Starch on Cellulose Studied by QCM-D. *Langmuir*, 24(9), 4743-4749.
- 522 Koppel, D. E. (1972). Analysis of Macromolecular Polydispersity in Intensity Correlation
523 Spectroscopy: The Method of Cumulants. *The Journal of Chemical Physics*, 57(11),
524 4814-4820.
- 525 Kronberg, B., Holmberg, K., & Lindman, B. (2014). *Adsorption of Polymers at Solid
526 Surfaces*. In *Surface Chemistry of Surfactants and Polymers* (pp. 211-229): John
527 Wiley & Sons, Ltd
- 528 Lee, S. H., Lee, H. L., & Youn, H. J. (2014). Adsorption and viscoelastic properties of
529 cationic xylan on cellulose film using QCM-D. *Cellulose*, 21(3), 1251-1260.
- 530 McCready, R. M., Guggolz, J., Silviera, V., & Owens, H. S. (1950). Determination of Starch
531 and Amylose in Vegetables. *Analytical Chemistry*, 22(9), 1156-1158.
- 532 Mohan, T., Niegelhell, K., Zarth, C. S. P., Kargl, R., Köstler, S., Ribitsch, V., Heinze, T.,
533 Spirk, S., & Stana-Kleinschek, K. (2014). Triggering Protein Adsorption on Tailored
534 Cationic Cellulose Surfaces. *Biomacromolecules*, 15(11), 3931-3941.
- 535 Mohan, T., Ristic, T., Kargl, R., Doliska, A., Köstler, S., Ribitsch, V., Marn, J., Spirk, S., &
536 Stana-Kleinschek, K. (2013). Cationically rendered biopolymer surfaces for high
537 protein affinity support matrices. *Chem. Comm.*, 49, 11530-11532.

538 Mohan, T., Spirk, S., Kargl, R., Doliška, A., Ehmman, H. M. A., Köstler, S., Ribitsch, V., &
539 Stana-Kleinschek, K. (2012). Watching cellulose grow – Kinetic investigations on
540 cellulose thin film formation at the gas–solid interface using a quartz crystal
541 microbalance with dissipation (QCM-D). *Colloids and Surfaces A: Physicochemical
542 and Engineering Aspects*, 400, 67-72.

543 Mohan, T., Spirk, S., Kargl, R., Doliska, A., Vesel, A., Salzmann, I., Resel, R., Ribitsch, V.,
544 & Stana-Kleinschek, K. (2012). Exploring the rearrangement of amorphous cellulose
545 model thin films upon heat treatment. *Soft Matter*, 8, 9807-9815.

546 Mohan, T., Zarth, C., Doliska, A., Kargl, R., Grießer, T., Spirk, S., Heinze, T., & Stana-
547 Kleinschek, K. (2013). Interactions of a cationic cellulose derivative with an ultrathin
548 cellulose support. *Carbohydr. Polym.*, 92, 1046-1053.

549 Nachtergaele, W. (1989). The Benefits of Cationic Starches for the Paper Industry. *Starch -
550 Stärke*, 41(1), 27-31.

551 Nechwatal, A., Michels, C., Kosan, B., & Nicolai, M. (2004). Lyocell blend fibers with
552 cationic starch: potential and properties. *Cellulose (Dordrecht, Neth.)*, 11(2), 265-272.

553 Niegelhell, K., Süßenbacher, M., Jammerneegg, K., Ganner, T., Schwendenwein, D., Schwab,
554 H., Stelzer, F., Plank, H., & Spirk, S. (2016). Enzymes as Biodevelopers for Nano-
555 And Micropatterned Bicomponent Biopolymer Thin Films. *Biomacromolecules*,
556 17(11), 3743-3749.

557 Orelma, H., Filpponen, I., Johansson, L.-S., Laine, J., & Rojas, O. J. (2011). Modification of
558 Cellulose Films by Adsorption of CMC and Chitosan for Controlled Attachment of
559 Biomolecules. *Biomacromolecules*, 12(12), 4311-4318.

560 Orelma, H., Johansson, L.-S., Filpponen, I., Rojas, O. J., & Laine, J. (2012). Generic Method
561 for Attaching Biomolecules via Avidin-Biotin Complexes Immobilized on Films of
562 Regenerated and Nanofibrillar Cellulose. *Biomacromolecules*, 13, 2802-2810.

563 Owens, D. K., & Wendt, R. C. (1969). Estimation of the surface free energy of polymers.
564 *Journal of Applied Polymer Science*, 13(8), 1741-1747.

565 Pérez, S., & Bertoft, E. (2010). The molecular structures of starch components and their
566 contribution to the architecture of starch granules: A comprehensive review. *Starch -
567 Stärke*, 62(8), 389-420.

568 Petersen, H., Radosta, S., Vorweg, W., & Kießler, B. (2013). Cationic starch adsorption onto
569 cellulosic pulp in the presence of other cationic synthetic additives. *Colloids and
570 Surfaces A: Physicochemical and Engineering Aspects*, 433, 1-8.

571 Rabel, W. (1971). Einige Aspekte Der Benetzungstheorie Und Ihre Anwendung Auf Die
572 Untersuchung Und Veränderung Der Oberflächeneigenschaften von Polymeren. *Farbe
573 und Lack*, 77, 997-1005.

574 Ristić, T., Mohan, T., Kargl, R., Hribernik, S., Doliška, A., Stana-Kleinschek, K., & Fras, L.
575 (2014). A study on the interaction of cationized chitosan with cellulose surfaces.
576 *Cellulose*, 21(4), 2315-2325.

577 Rohm, S., Hirn, U., Ganser, C., Teichert, C., & Schennach, R. (2014). Thin cellulose films as
578 a model system for paper fibre bonds. *Cellulose*, 21(1), 237-249.

579 Rosin, P. M., Lajolo, F. M., & Menezes, E. W. (2002). Measurement and Characterization of
580 Dietary Starches. *Journal of Food Composition and Analysis*, 15(4), 367-377.

581 Schaub, M., Wenz, G., Wegner, G., Stein, A., & Klemm, D. (1993). Ultrathin films of
582 cellulose on silicon wafers. *Advanced Materials*, 5(12), 919-922.

583 Schnablegger, H., & Glatter, O. (1991). Optical sizing of small colloidal particles: an
584 optimized regularization technique. *Applied Optics*, 30(33), 4889-4896.

585 Schwikal, K., Heinze, T., Saake, B., Puls, J., Kaya, A., & Esker, A. R. (2011). Properties of
586 spruce sulfite pulp and birch kraft pulp after sorption of cationic birch xylan.
587 *Cellulose*, 18, 727–737.

- 588 Shirazi, M., van de Ven, T. G. M., & Garnier, G. (2003a). Adsorption of Modified Starches
589 on Porous Glass. *Langmuir*, 19(26), 10829-10834.
- 590 Shirazi, M., van de Ven, T. G. M., & Garnier, G. (2003b). Adsorption of Modified Starches
591 on Pulp Fibers. *Langmuir*, 19(26), 10835-10842.
- 592 Steeneken, P. A. M., & Smith, E. (1991). Topochemical effects in the methylation of starch.
593 *Carbohydrate Research*, 209, 239-249.
- 594 Strasser, S., Niegellhell, K., Kaschowitz, M., Markus, S., Kargl, R., Stana-Kleinschek, K.,
595 Slugovc, C., Mohan, T., & Spirk, S. (2016). Exploring Nonspecific Protein Adsorption
596 on Lignocellulosic Amphiphilic Bicomponent Films. *Biomacromolecules*, 17(3),
597 1083-1092.
- 598 Swerin, A., & Wågberg, L. (1994). Size-exclusion chromatography for characterization of
599 cationic polyelectrolytes used in papermaking. *Nordic Pulp & Paper Research*
600 *Journal*, 09(1), 018-025.
- 601 Tammelin, T., Merta, J., Johansson, L.-S., & Stenius, P. (2004). Viscoelastic Properties of
602 Cationic Starch Adsorbed on Quartz Studied by QCM-D. *Langmuir*, 20, 10900-10909.
- 603 Tammelin, T., Saarinen, T., Österberg, M., & Laine, J. (2006). Preparation of
604 Langmuir/Blodgett-cellulose Surfaces by Using Horizontal Dipping Procedure.
605 Application for Polyelectrolyte Adsorption Studies Performed with QCM-D.
606 *Cellulose*, 13(5), 519.
- 607 Terada, E., Samoshina, Y., Nylander, T., & Lindman, B. (2004a). Adsorption of Cationic
608 Cellulose Derivative/Anionic Surfactant Complexes onto Solid Surfaces. II.
609 Hydrophobized Silica Surfaces. *Langmuir*, 20, 6692-6701.
- 610 Terada, E., Samoshina, Y., Nylander, T., & Lindman, B. (2004b). Adsorption of Cationic
611 Cellulose Derivatives/Anionic Surfactant Complexes onto Solid Surfaces. I. Silica
612 Surfaces. *Langmuir*, 20, 1753-1762.
- 613 Theisen, A., Johann, C., Deacon, M., & Harding, S. (2000). *Refractive Increment Data-Book*
614 *for Polymer and Biomolecular Scientists*: Nottingham University Press.
- 615 Yokota, S., Kitaoka, T., & Wariishi, H. (2007). Surface morphology of cellulose films
616 prepared by spin coating on silicon oxide substrates pretreated with cationic
617 polyelectrolyte. *Applied Surface Science*, 253(9), 4208-4214.

618